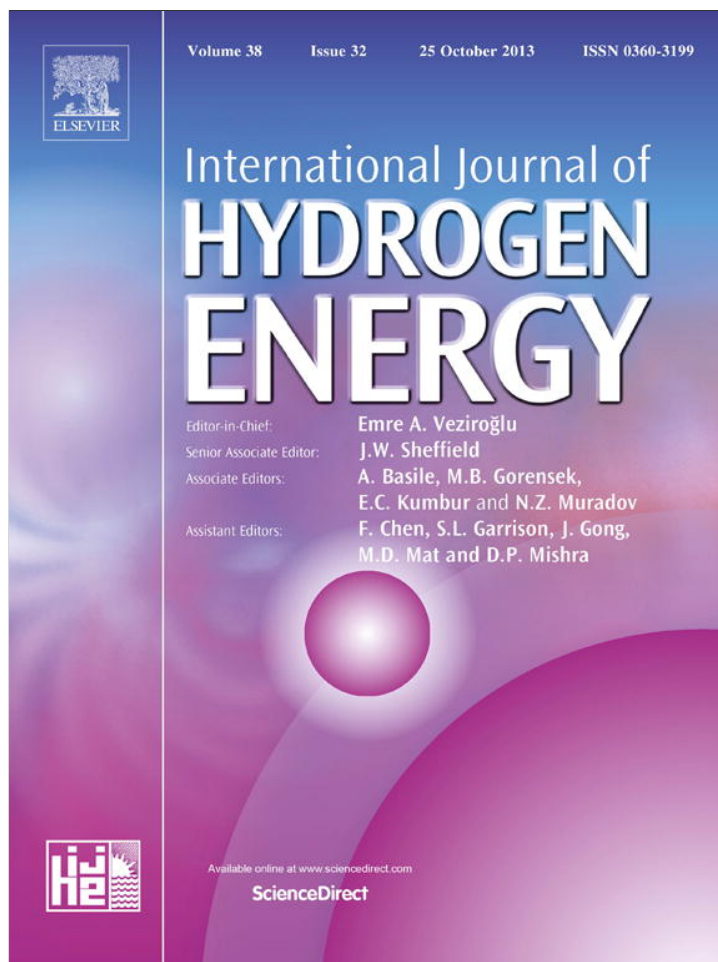


Provided for non-commercial research and education use.
Not for reproduction, distribution or commercial use.



This article appeared in a journal published by Elsevier. The attached copy is furnished to the author for internal non-commercial research and education use, including for instruction at the authors institution and sharing with colleagues.

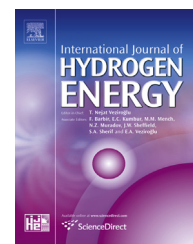
Other uses, including reproduction and distribution, or selling or licensing copies, or posting to personal, institutional or third party websites are prohibited.

In most cases authors are permitted to post their version of the article (e.g. in Word or Tex form) to their personal website or institutional repository. Authors requiring further information regarding Elsevier's archiving and manuscript policies are encouraged to visit:

<http://www.elsevier.com/authorsrights>

Available online at www.sciencedirect.com

SciVerse ScienceDirect

journal homepage: www.elsevier.com/locate/he

Mathematical modeling of alkaline direct ethanol fuel cells

L. An, Z.H. Chai, L. Zeng, P. Tan, T.S. Zhao*

Department of Mechanical Engineering, The Hong Kong University of Science and Technology, Clear Water Bay, Kowloon, Hong Kong Special Administrative Region, China

ARTICLE INFO

Article history:

Received 24 June 2013

Received in revised form

8 August 2013

Accepted 19 August 2013

Available online 14 September 2013

Keywords:

Fuel cell

Alkaline direct ethanol fuel cell

Mathematical modeling

Mass transport

Activation polarization

ABSTRACT

A one-dimensional model is developed for alkaline direct ethanol fuel cells (DEFC) by considering the complicated physicochemical processes, including mass transport, charge transport, and electrochemical reactions. The model is validated against experiments and shows good agreement with the literature data. The model is then used to investigate the effects of various operating and structural design parameters on the cell performance. Numerical results show that the cell performance increases with increasing the ethanol concentration from 1.0 M to 3.0 M and with increasing the OH⁻ concentration from 1.0 M to 5.0 M. The model is further applied to the study of the effect of the design of the anode diffusion layer (DL) on the performance; it is shown that the cell performance improves when the porosity of the DL is increased and the thickness of the DL is decreased.

Copyright © 2013, Hydrogen Energy Publications, LLC. Published by Elsevier Ltd. All rights reserved.

1. Introduction

Alkaline direct ethanol fuel cells (DEFCs), which promise to be a clean and efficient energy production technology, have recently attracted worldwide attention, primarily because ethanol is a carbon-neutral, sustainable fuel and possesses many unique physicochemical properties including high energy density and ease of transportation, storage as well as handling [1–3]. The conventional architecture design of alkaline DEFC systems is similar to that of proton exchange membrane (PEM) fuel cells, in which the ion transport pathways between the anode and cathode are formed by the network of dispersed ionomers in the electrodes that are interfaced with the membrane [4]. However, such a fuel cell system that purely relies on an anion-exchange membrane (AEM) to conduct ions through the membrane and ionomers in the electrodes exhibits extremely low cell performance (the

state-of-the-art peak power density is 1.6 mW cm⁻² at 60 °C) [5], primarily because of the low conductivity of state-of-the-art AEMs and ionomers. For this reason, past efforts with respect to the AEM-DEFCs have mainly been made to the development of high-conductivity AEMs and ionomers, as well as highly-catalytic materials for both the ethanol oxidation reaction (EOR) and oxygen reduction reaction (ORR) [6,7]. Recently, it has been demonstrated that, even using existing ion conductors and catalysts, adding an alkali (e.g.: NaOH/KOH) to ethanol would improve the performance of AEM-DEFCs (the state-of-the-art peak power density can be as high as 185 mW cm⁻² at 60 °C) [8]. Such a breakthrough can be attributed to the added base, which not only dramatically increases the ionic conductivity of the membranes [9,10], but also enables the kinetics of the EOR to be further sped up [11,12]. As the involvement of an alkali creates a new alkaline DEFC system and makes the physicochemical processes more

* Corresponding author. Tel.: +852 2358 8647.

E-mail address: metzhao@ust.hk (T.S. Zhao).

0360-3199/\$ – see front matter Copyright © 2013, Hydrogen Energy Publications, LLC. Published by Elsevier Ltd. All rights reserved.

<http://dx.doi.org/10.1016/j.ijhydene.2013.08.080>

Table 1 – Physicochemical parameters.

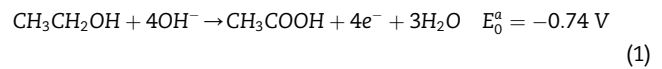
Parameter	Symbol	Value	Unit	Ref.
Anode standard potential	E_0^a	-0.74	V	[11]
Cathode standard potential	E_0^c	0.40	V	[11]
Anode transfer coefficient	α_a	0.5	–	Assumed
Cathode transfer coefficient	α_c	0.5	–	Assumed
Anode exchange current density	$i_{0,a}$	50	$A\ m^{-2}$	[13]
Cathode exchange current density	$i_{0,c}$	44	$A\ m^{-2}$	[13]
Universal gas constant	R	8.314	$J\ mol^{-1}\ K^{-1}$	
Faraday's constant	F	96485.3	$A\ s\ mol^{-1}$	
Number of anode transferred electrons	n_a	4	–	
Number of cathode transferred electrons	n_c	4	–	

complicated, including mass transport, charge (ionic and electronic) transport, and electrochemical reactions, it is difficult to shed light on the physicochemical processes through experimental investigations. On the other hand, the mathematical modeling, as a powerful and economical tool, may play an important role in quantifying the complicated physicochemical processes in alkaline DEFCs. Recently, Bahrami and Faghri [13] developed a one-dimensional, isothermal, multi-layer membrane model to investigate the mass transport in the alkaline DEFC, which incorporates the diffusive and electroosmotic transport of ethanol through the membrane; they found that the ethanol crossover is significantly reduced upon using an anion exchange membrane instead of a proton exchange membrane, particularly at high current densities [13]. However, the effect of an added base on the cell performance (ionic transport and electrochemical kinetics) was not considered, which has been shown to have a significant influence on cell performance [14,15]. In this work, we present a theoretical model that incorporates integrated mass transport, charge transport, and electrochemical reactions. The model allows the effects of various operating and structural design parameters, including the species concentration and the porosity and thickness of the anode diffusion layer (DL), on the cell performance to be examined.

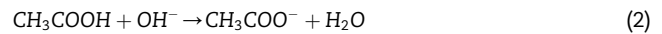
2. Formulation

Consider an alkaline DEFC, as shown in Fig. 1, which consists of an anode flow field (FF), an anode DL, an anode catalyst layer (CL), an anion exchange membrane (AEM), a cathode CL,

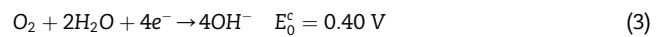
a cathode DL and a cathode FF. On the anode, the fuel-electrolyte-mixed solution (ethanol and alkali) flowing into the anode FF is transported through the anode DL to the anode CL, where ethanol is oxidized to generate electrons, water, and acetic acid [16]:



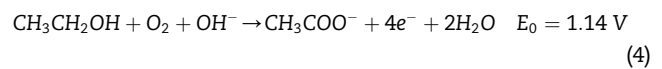
The acetic acid produced by the electro-oxidation of ethanol will combine with OH^- to form acetate according to:



The water in fuel solution, along with that produced from the EOR, diffuses through the membrane to the cathode CL, while the produced electrons pass through an external electrical load to the cathode. On the cathode, the oxygen/air is transported through the cathode DL to the cathode CL, where oxygen combines with electrons and water from the anode to produce OH^- ions according to:



Subsequently, the generated OH^- ions are conducted through the membrane to the anode for the EOR. Therefore, combining Eqs. (1)–(3) results in an overall reaction for the alkaline DEFC:



It is clear from the above description that operating an alkaline DEFC actually involves rather complex transport processes coupled with electrochemical reactions of both the

Table 2 – Operating parameters.

Parameter	Symbol	Value	Unit	Ref.
Operating temperature	T	333.15	K	
Gas pressure	P	1.013×10^{-5}	Pa	
Inlet concentration of CH_3COO^-	$C_{CH_3COO^-}^{inlet}$	0	$mol\ m^{-3}$	Assumed
Inlet concentration of O_2 (air)	$C_{O_2, Air}^{inlet}$	$0.21 \times P/(RT)$	$mol\ m^{-3}$	[24]
Inlet concentration of O_2 (pure oxygen)	$C_{O_2, Pure}^{inlet}$	$P/(RT)$	$mol\ m^{-3}$	[24]
Reference O_2 concentration	$C_{O_2}^{ref}$	$P/(RT)$	$mol\ m^{-3}$	[24]
Reference ethanol concentration	C_{EtOH}^{ref}	3000	$mol\ m^{-3}$	[20]
Reference OH^- concentration	$C_{OH^-}^{ref}$	5000	$mol\ m^{-3}$	[20]

Table 3 – Structural parameters.

Parameter	Symbol	Value	Unit	Ref.
Porosity of anode DL	ϵ_{ADL}	0.95	–	[25]
Thickness of anode DL	l_{ADL}	1.0×10^{-3}	m	Measured
Thickness of membrane	l_M	2.8×10^{-5}	m	[12]
Porosity of cathode DL	ϵ_{ACL}	0.73	–	[26]
Thickness of cathode DL	l_{CDL}	2.0×10^{-4}	m	Measured
Contact resistance	$R_{contact}$	2.0×10^{-5}	$\Omega \text{ m}^2$	[17]

ethanol oxidation on the anode and the oxygen reduction on the cathode. To make the complicated process tractable, we develop a one-dimensional model (x axis: through-plane direction) with the following simplifications and assumptions:

- (1) The fuel cell is assumed to operate under steady-state and isothermal conditions.
- (2) The mass/charge transport through DLs is assumed to be a diffusion-predominated process and the convection effect due to bulk flow is ignored.
- (3) Each CL is treated as an interface since it is much thinner than DLs and membrane.
- (4) Ethanol and alkali crossover through the membrane are ignored.

It should be mentioned that unlike in the acid direct methanol fuel cells (DMFC), on one hand, the ethanol crossover rate in alkaline DEFCs is smaller than the methanol crossover rate in acid DMFCs [12]. On the other hand, the ethanol crossover in alkaline DEFCs only causes the fuel loss, rather than the mixed potential (ethanol tolerant catalysts used at the cathode) [1].

2.1. Mass transport

On the anode, the mass conservation is expressed as:

$$\nabla N_i = 0 \quad (5)$$

where the species flux (N_i) is related to the concentration gradient based on the Fick's law:

$$N_i = -D_i^{eff} \frac{dC_i}{dx} \quad (6)$$

where C stands for the species concentration, and the effective diffusivity of species, D_i^{eff} , (i : ethanol, OH^- , CH_3COO^-) is given by [17]:

Table 4 – Mass/charge transport parameters.

Parameter	Symbol	Value	Unit	Ref.
Diffusivity of Na^+	D_{Na^+}	1.33×10^{-9}	$\text{m}^2 \text{ s}^{-1}$	[27]
Diffusivity of OH^-	D_{OH^-}	5.26×10^{-9}	$\text{m}^2 \text{ s}^{-1}$	[27]
Diffusivity of CH_3COO^-	$D_{\text{CH}_3\text{COO}^-}$	1.09×10^{-9}	$\text{m}^2 \text{ s}^{-1}$	[27]
Diffusivity of ethanol	D_{EtOH}	6.00×10^{-9}	$\text{m}^2 \text{ s}^{-1}$	[28]
Diffusivity of O_2	$D_{\text{O}_2, \text{Air}}$	$1.775 \times 10^{-5} \times (T/273.15)^{1.823}$	$\text{m}^2 \text{ s}^{-1}$	[17]
Conductivity of membrane	σ_M	5.5	$\Omega^{-1} \text{ m}^{-1}$	[12]

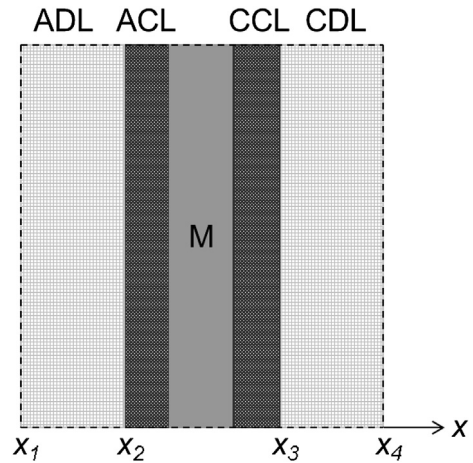


Fig. 1 – Schematic of an alkaline DEFC and the coordinate system.

$$D_i^{eff} = \epsilon^{z_i} D_i \quad (7)$$

The electroneutrality of the fuel-electrolyte-mixed solution is followed by:

$$\sum_i z_i C_i = 0 \quad (8)$$

where z represents the valence for ions and i stands for Na^+ , OH^- and CH_3COO^- .

On the cathode, oxygen extracted from the air reacts with the electron and water to produce the OH^- ions. The mass conservation of oxygen reads:

$$\nabla N_{\text{O}_2} = 0 \quad (9)$$

where the oxygen flux (N_{O_2}) is proportional to the concentration gradient according to the Fick's law:

$$N_{\text{O}_2} = -D_{\text{O}_2}^{eff} \frac{dC_{\text{O}_2}}{dx} \quad (10)$$

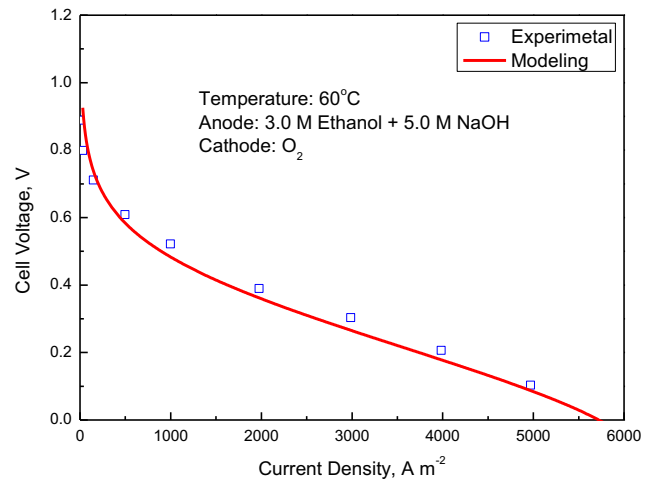


Fig. 2 – Comparison between the numerical results and experimental data [18].

where the effective diffusivity of O_2 , $D_{O_2}^{eff}$, is given by [17]:

$$D_{O_2}^{eff} = \varepsilon^{\frac{2}{3}} D_{O_2} \quad (11)$$

It should be noted that for the case of using pure oxygen on the cathode, we assume that the cathode is fully filled by the oxygen, i.e.:

$$C_{O_2} = C_{O_2}^{inlet} \quad (12)$$

2.2. Electrochemical kinetics

On the anode, the electro-oxidation of ethanol is a complicated multi-step electrochemical process, and its reaction mechanism is yet to be completely understood. To simplify the problem, a Tafel-form kinetics for the EOR considering the mass-transfer effect of reactants is applied:

$$j_a = i_{0,a} \left(\frac{C_{EtOH}^{ACL}}{C_{EtOH}^{ref}} \right)^{\gamma_a^{EtOH}} \left(\frac{C_{OH^-}^{ACL}}{C_{OH^-}^{ref}} \right)^{\gamma_a^{OH^-}} \exp\left(\frac{\alpha_a F}{RT} \eta_a\right) \quad (13)$$

$$\gamma_a^{EtOH} = \begin{cases} 0 & C_{EtOH}^{ACL} > C_{EtOH}^{ref} \\ 1 & C_{EtOH}^{ACL} \leq C_{EtOH}^{ref} \end{cases} \quad (14)$$

$$\gamma_a^{OH^-} = \begin{cases} 0 & C_{OH^-}^{ACL} > C_{OH^-}^{ref} \\ 1 & C_{OH^-}^{ACL} \leq C_{OH^-}^{ref} \end{cases} \quad (15)$$

where C_i^{ACL} is the species concentration in the anode CL and C_i^{ref} is the reference concentration of species. The reaction order γ is related to the species concentration and is assumed to be zero-order when its concentration is higher than a reference value. Otherwise, a first-order reaction is specified.

With respect to the electro-reduction of oxygen on the cathode, a Tafel-form kinetics is employed:

$$j_c = i_{0,c} \left(\frac{C_{O_2}^{CCL}}{C_{O_2}^{ref}} \right)^{\gamma_c} \exp\left(\frac{\alpha_c F}{RT} \eta_c\right) \quad (16)$$

$$\gamma_c = \begin{cases} 0 & C_{O_2}^{CCL} > C_{O_2}^{ref} \\ 1 & C_{O_2}^{CCL} \leq C_{O_2}^{ref} \end{cases} \quad (17)$$

where $C_{O_2}^{CCL}$ is the oxygen concentration in the cathode CL and $C_{O_2}^{ref}$ is the reference concentration of oxygen.

2.3. Boundary conditions

On the anode,

$$x = x_1 : C_i = C_i^{inlet} \quad (i : \text{ethanol, Na}^+, \text{OH}^-, \text{CH}_3\text{COO}^-) \quad (18)$$

$$x = x_2 : N_i = \frac{i_{cell} S_i}{n_i F} \quad (i : \text{ethanol, OH}^-, \text{CH}_3\text{COO}^-) \quad (19)$$

On the cathode,

$$x = x_3 : N_{O_2} = \frac{i_{cell} S_{O_2}}{n_c F} \quad (20)$$

$$x = x_4 : C_{O_2} = C_{O_2}^{inlet} \quad (21)$$

2.4. Cell voltage

With the anode and cathode overpotentials obtained from the equations presented above, we can assess the cell voltage:

$$V_{cell} = E_0 - \eta_a - \eta_c - i_{cell} \left(R_{contact} + \frac{l_M}{\sigma_M} \right) \quad (22)$$

where E_0 is the theoretical potential of the alkaline DEFC, and the cell resistance is composed of the contact resistance ($R_{contact}$) and the membrane resistance (l_M/σ_M).

The physicochemical, operating, structural, and mass/charge transport parameters are listed in Tables 1–4, respectively.

3. Results and discussion

3.1. Model validation

The numerical results of the polarization behavior and experimental data are compared in Fig. 2. The experimental data were collected when the alkaline DEFC was operated at

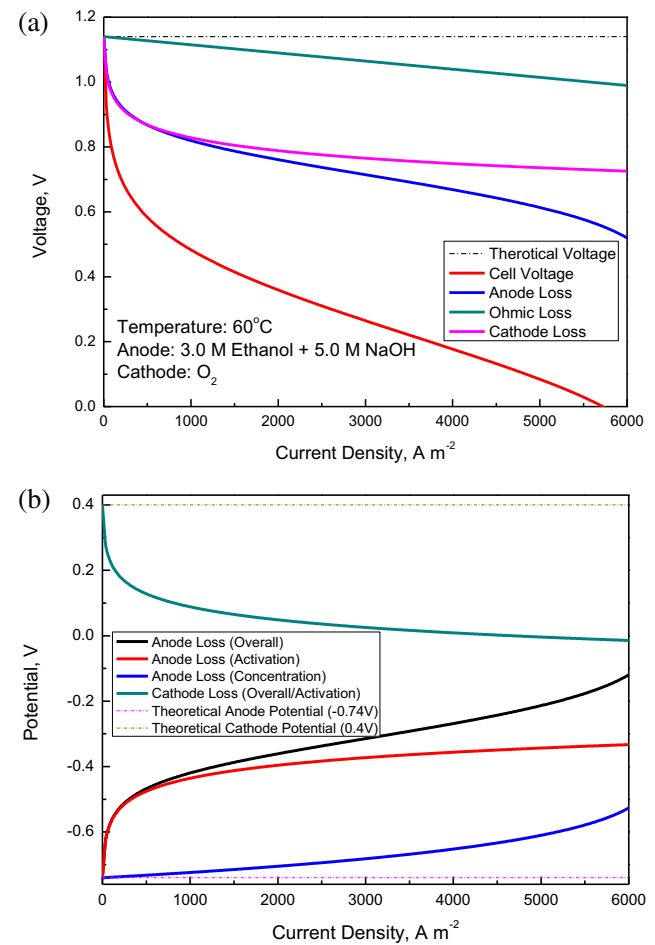


Fig. 3 – Specific loss with the current density. (a) Voltage loss; (b) potential loss.

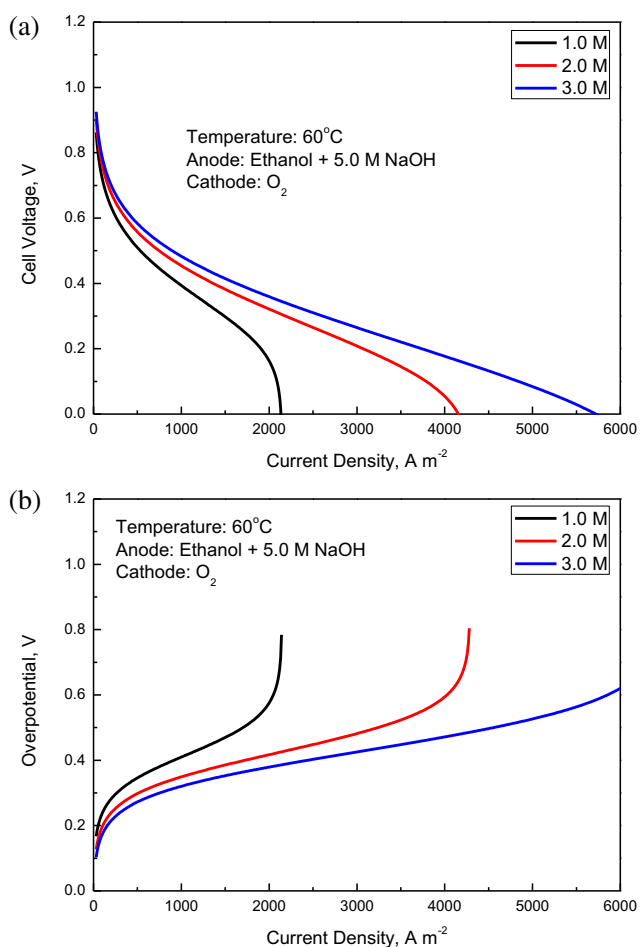


Fig. 4 – Effect of the ethanol concentration on the cell performance. (a) Polarization curves; (b) Anode overpotentials.

60 °C with a fuel-electrolyte-mixed solution (5.0 M ethanol + 3.0 M NaOH) at the anode and pure oxygen at the cathode [18]. It is seen that the predicted polarization curve is in good agreement with the experimental data. In the following, we will present the numerical results on the effects of operating and structural design parameters on the cell performance.

3.2. Voltage/potential loss

Fig. 3a shows the anode overpotential, cathode overpotential, the ohmic loss, and the overall polarization curve. Generally, the anode/cathode overpotential results from the activation polarization and the concentration polarization, while the ohmic loss is associated with the ionic and electronic transport resistance [19]. It can be also found that the largest polarization appears on the anode, indicating that the major loss in the alkaline DEFC is the anode polarization, which is consistent with the previous investigation [20]. More clearly, Fig. 3b presents the decoupled activation and concentration polarizations for the anode and cathode, respectively. It can be seen that the anode and cathode losses are predominated by the activation loss, particularly for the cathode loss. It

should be noticed from Fig. 3b that the cathode loss is completely attributed to the activation loss, which is due to the use of pure oxygen. The predicted results suggest that although the added alkali much improves the EOR kinetics [5], the electro-oxidation of ethanol on the existing catalysts still causes a large activation polarization [21].

3.3. Effect of the species concentration

3.3.1. Ethanol

Fig. 4a shows the effect of various ethanol concentrations on the cell performance. It can be seen that increasing the ethanol concentration from 1.0 M to 3.0 M increases the cell voltage. The improvement in performance is attributed in part to the enhanced kinetics of the EOR, which is evident from the anode overpotential shown in Fig. 4b, and in part to the fast delivery rate of ethanol to the anode CL, which is evident from the ethanol concentration in the anode CL shown in Fig. 5. A lower ethanol concentration in the anode CL leads to the large activation loss, as shown in Fig. 4. On the other hand, the lower ethanol concentration also causes the large concentration polarization in the high current density region, as shown by the results in Fig. 5. For instance, the limiting current density appears in the case of the 1.0-M and 2.0-M operations, which is obviously caused by the mass transport limitation of ethanol, as seen from Fig. 5. However, the 3.0-M operation does not show the mass transport limitation in the whole current density region. When the cell voltage becomes zero, the ethanol concentration in the anode CL is still larger than zero, as shown in Figs. 4 and 5, indicating that the mass transfer rate of ethanol is larger than the reaction rate and thus the mass transport limitation will not take place.

3.3.2. Alkali

Fig. 6a shows the effect of the alkali concentration on the cell performance. It can be seen that by increasing the alkali concentration from 1.0 M to 5.0 M, the cell performance increases in the whole current density region. This is because increasing the alkali concentration not only improves the EOR kinetics (see Fig. 6b), but also fastens the transfer rate of OH⁻ ions to the reaction sites (see Fig. 7). We also note that, as

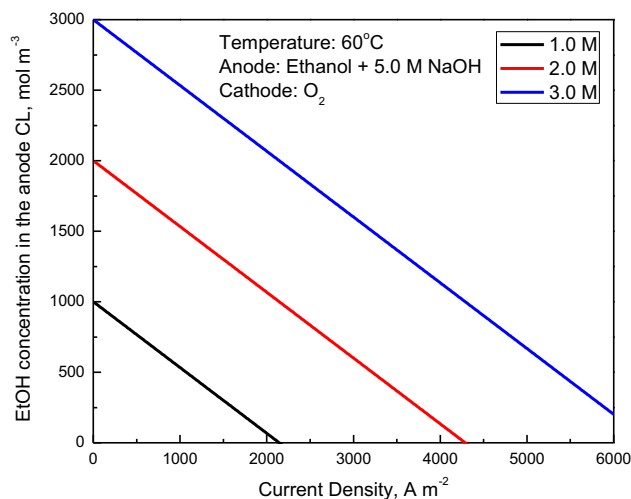


Fig. 5 – The ethanol concentration in the anode CL.

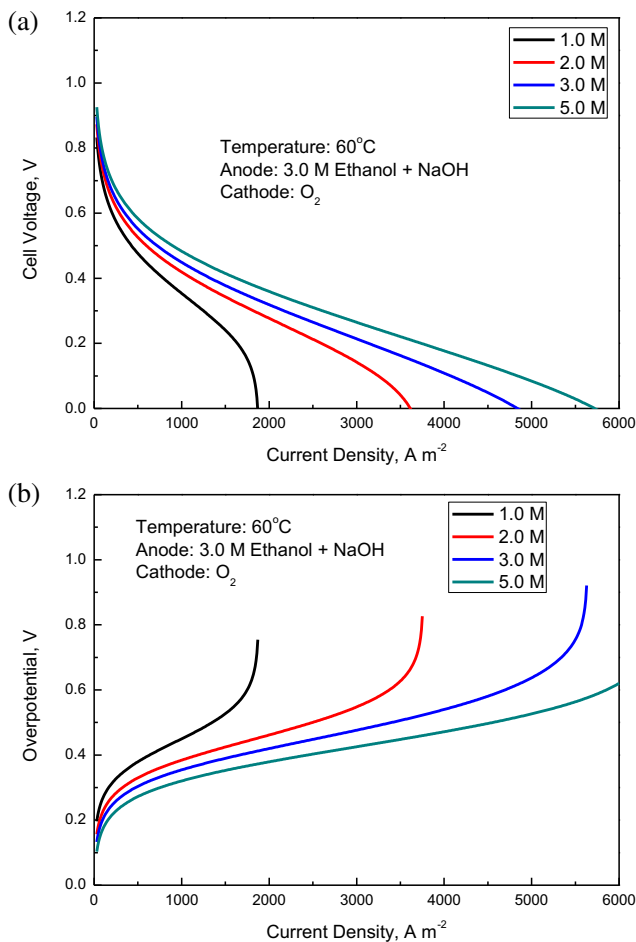


Fig. 6 – Effect of the alkali concentration on the cell performance. (a) Polarization curves; (b) Anode overpotentials.

shown in Figs. 6 and 7, too low of an alkali concentration will cause the large activation loss at low current densities, and the large concentration loss in the high current density region. For example, it is seen from Fig. 7 that the limiting current density appears in the case of the 1.0-M and 2.0-M operations, which is obviously caused by the mass transport limitation of OH⁻ ions. However, the 3.0-M and 5.0-M operations do not show the limiting current density, although the 3.0-M operation would show the mass transport limitation at about 5500 A m⁻². When the cell is exhausted (the voltage becomes zero), the OH⁻ concentration at the anode CL is still larger than zero, as shown in Figs. 6 and 7, indicating that for the 3.0-M and 5.0-M operations, the mass transfer rate of OH⁻ ions is higher than the reaction rate and thus the mass transport limitation does not take place.

3.4. Effect of the oxygen concentration

Oxygen is transported through the gas pores from the cathode channel to the cathode CL, in which the oxygen concentration becomes lower due to the consumption of oxygen by the ORR. With an increase in the current density, the oxygen

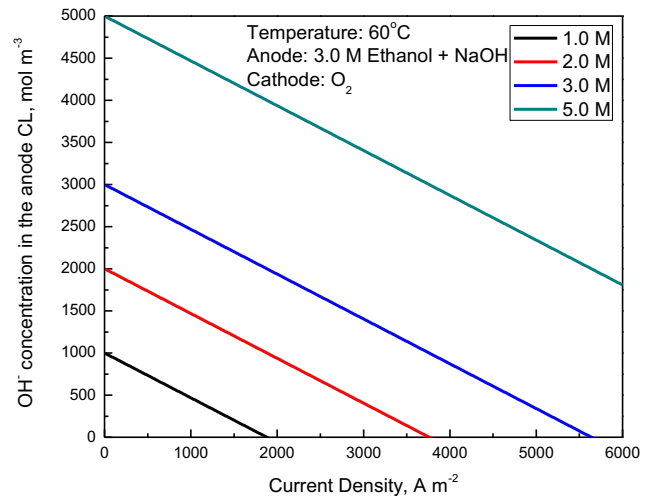


Fig. 7 – The alkali concentration in the anode CL.

concentration is also reduced due to the increased oxygen consumption rate. However, the decrease in the oxygen concentration from the channel to the CL is relatively small even at high current densities, indicating that the mass transport

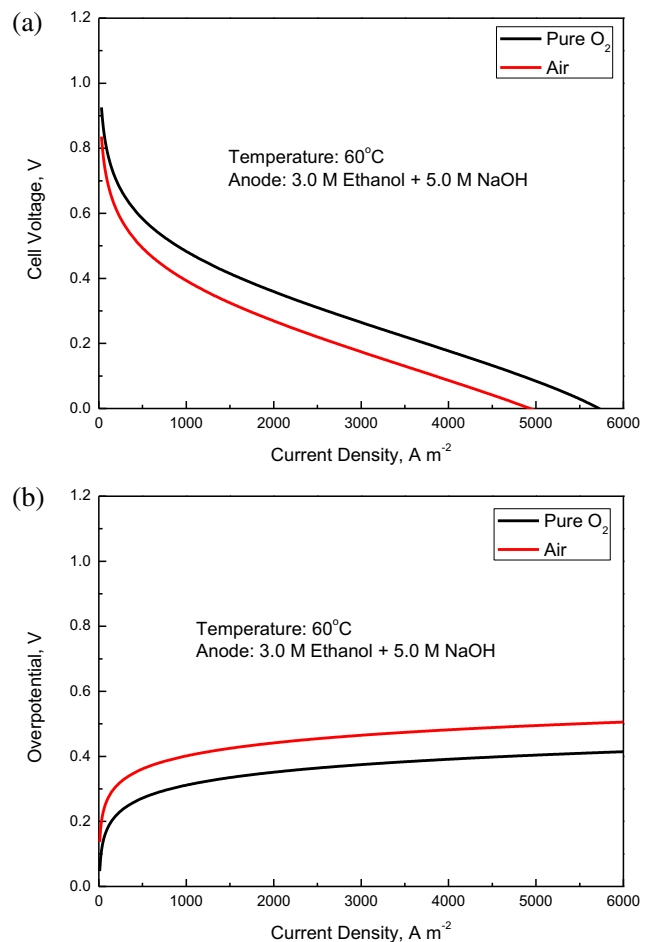


Fig. 8 – Effect of the oxygen concentration on the cell performance. (a) Polarization curves; (b) Cathode overpotentials.

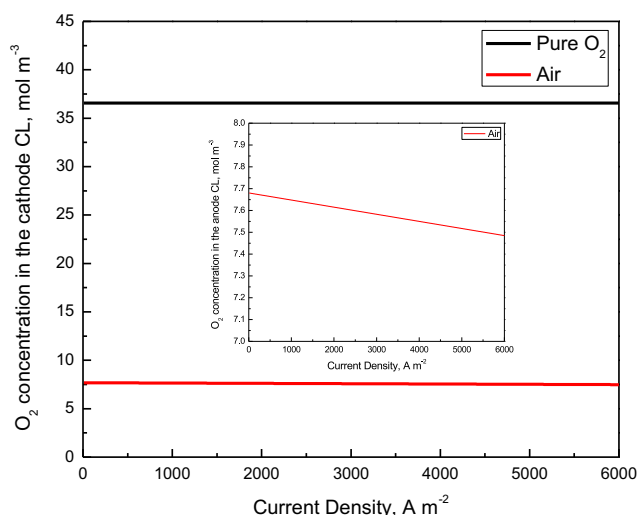


Fig. 9 – The oxygen concentration in the cathode CL.

resistance of oxygen is rather low [22]. This is due to the fast delivery rate of oxygen in the gas phase. Experimentally, the cell was operated with the pure oxygen to avoid the negative effect of the presence of CO_2 in the alkaline DEFC system. In a real case, however, the air is generally used, although the pre-removal of CO_2 is needed. For this reason, we compared the polarization curves and cathode overpotentials as operated with the pure oxygen and the air, respectively. It can be seen from Fig. 8a that the cell voltage with the pure oxygen is higher than that operated with the air over the whole current density region, which is consistent with the previous investigation [23]. The higher oxygen concentration yields faster kinetics as compared to the air, resulting in a lower activation loss evident from the cathode overpotential shown in Fig. 8b. The oxygen concentration in the cathode CL is almost the same with that in the inlet, as shown in Fig. 9, indicating the mass transfer rate of oxygen is high enough to match the reaction rate.

3.5. Effect of the anode DL design parameters

We also investigated the effect of the anode structural design parameters (DL thickness and porosity) on the cell performance. Generally, the anode DL thickness and porosity strongly influence the mass transport resistance of the reactant/product. It is seen from Fig. 10a that with increasing the anode DL from 0.5 mm to 2.0 mm, the cell performance gradually decreases, which is due to the fact that the thicker DL increases the mass transport resistance of species, i.e.: lower reactant delivery rate and product removal rate. Therefore, from the mass transfer point of view, the thinner anode DL is preferred as a result of the fast reactant delivery and product removal. As for the porosity, it is found that increasing the porosity from 73% to 98%, the mass/charge transport is enhanced, as shown in Fig. 10b. This is because the smaller porosity has a higher mass/charge transport resistance through the porous media. For this reason, the nickel foam with a porosity of 95% is generally used as the DL in alkaline DEFCs. On the other hand, the DL functions as not

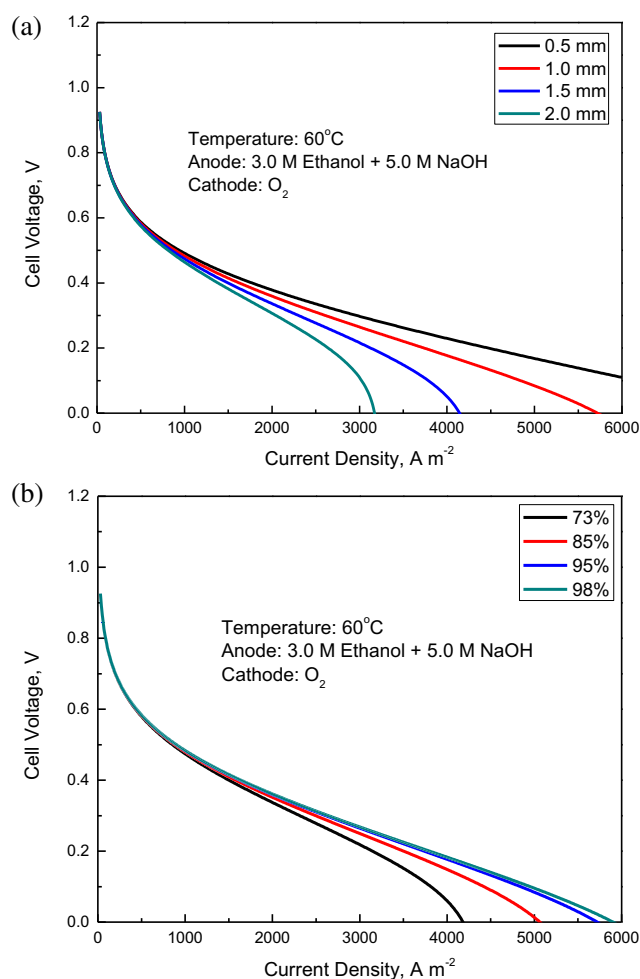


Fig. 10 – Effect of the anode DL parameters on the cell performance. (a) Thickness; (b) Porosity.

only a reactant distributor, but also an electron transmitter and a CL supporter. A higher porosity means the larger electron transport resistance and the worse mechanical property. In a real case, therefore, the positive effect of the low mass transport resistance and the negative effect of the high electron transport resistance and the poor mechanical property will result in an optimal porosity for the DLs.

4. Concluding remarks

We have developed a one-dimensional mathematical model that incorporates the coupled mass transport, charge transport, and electrochemical reaction occurring in the alkaline DEFC. It has been demonstrated that the results of the model are in good agreement with the literature experimental data. The numerical results suggest that the major voltage loss in the alkaline DEFC results from the anode polarization, primarily due to the sluggish EOR kinetics. It is also shown that the cell performance improves with increasing the reactant concentration, primarily due to the increased mass transfer rate of reactants and the decreased activation loss of the electrochemical reaction. Furthermore, the effects of the

design parameters of the anode DL are examined; the results show that the cell performance increases with increasing the DL porosity, but with decreasing the DL thickness as a result of the increased mass transfer rate.

Acknowledgments

The work described in this paper was fully supported by a grant from the Research Grants Council of the Hong Kong Special Administrative Region, China (Project No. HKUST9/CRF/11G).

REFERENCES

- [1] Zhao TS, Li YS, Shen SY. Anion-exchange membrane direct ethanol fuel cells: status and perspectives. *Front Energy Power Eng China* 2010;4:443–58.
- [2] Antolini E, Gonzalez ER. Alkaline direct alcohol fuel cells. *J Power Sources* 2010;195:3431–50.
- [3] Yu EH, Wang X, Krewer U, Li L, Scott K. Direct oxidation alkaline fuel cells: from materials to systems. *Energy Environ Sci* 2012;5:5668–80.
- [4] Wang Y, Chen KS, Mishler J, Cho SC, Adroher XC. A review of polymer electrolyte membrane fuel cells: technology, applications, and needs on fundamental research. *Appl Energy* 2011;88:981–1007.
- [5] Li YS, Zhao TS, Liang ZX. Effect of polymer binders in anode catalyst layer on performance of alkaline direct ethanol fuel cells. *J Power Sources* 2009;190:223–9.
- [6] Varcoe JR, Slade RCT. Prospects for alkaline anion-exchange membranes in low temperature fuel cells. *Fuel Cells* 2005;5:187–200.
- [7] Bianchini C, Shen PK. Palladium-based electrocatalysts for alcohol oxidation in half cells and in direct alcohol fuel cells. *Chem Rev* 2009;109:4183–206.
- [8] Xu JB, Zhao TS, Li YS, Yang WW. Synthesis and characterization of the Au-modified Pd cathode catalyst for alkaline direct ethanol fuel cells. *Int J Hydrogen Energy* 2010;35:9693–700.
- [9] An L, Zhao TS, Shen SY, Wu QX, Chen R. Performance of a direct ethylene glycol fuel cell with an anion-exchange membrane. *Int J Hydrogen Energy* 2010;35:4329–35.
- [10] An L, Zhao TS, Shen SY, Wu QX, Chen R. An alkaline direct oxidation fuel cell with non-platinum catalysts capable of converting glucose to electricity at high power output. *J Power Sources* 2011;196:186–90.
- [11] An L, Zhao TS, Chen R, Wu QX. A novel direct ethanol fuel cell with high power density. *J Power Sources* 2011;196:6219–22.
- [12] An L, Zhao TS, Wu QX, Zeng L. Comparison of different types of membrane in alkaline direct ethanol fuel cells. *Int J Hydrogen Energy* 2012;37:14536–42.
- [13] Bahrami H, Faghri A. Multi-layer membrane model for mass transport in a direct ethanol fuel cell using an alkaline anion exchange membrane. *J Power Sources* 2012;218:286–96.
- [14] An L, Zhao TS, Xu JB. A bi-functional cathode structure for alkaline-acid direct ethanol fuel cells. *Int J Hydrogen Energy* 2011;36:13089–95.
- [15] An L, Zhao TS, Li YS, Wu QX. Charge carriers in alkaline direct oxidation fuel cells. *Energy Environ Sci* 2012;5:7536–8.
- [16] An L, Zhao TS, Zeng L. Agar chemical hydrogel electrode binder for fuel-electrolyte-fed fuel cells. *Appl Energy* 2013;109:67–71.
- [17] Yang WW, Zhao TS. A two-dimensional, two-phase mass transport model for liquid-feed DMFCs. *Electrochim Acta* 2007;52:6125–40.
- [18] An L, Zhao TS. An alkaline direct ethanol fuel cell with a cation exchange membrane. *Energy Environ Sci* 2011;4:2213–7.
- [19] Larmine J, Dicks A. *Fuel cell systems explained*. 2nd ed. West Sussex: Wiley; 2003.
- [20] Li YS, Zhao TS, Liang ZX. Performance of alkaline electrolyte-membrane based direct ethanol fuel cells. *J Power Sources* 2009;187:387–92.
- [21] An L, Zhao TS. Performance of an alkaline-acid direct ethanol fuel cell. *Int J Hydrogen Energy* 2011;36:9994–9.
- [22] Xu C, Zhao TS, Yang WW. Modeling of water transport through the membrane electrode assembly for direct methanol fuel cells. *J Power Sources* 2008;178:291–308.
- [23] An L, Zeng L, Zhao TS. An alkaline direct ethylene glycol fuel cell with an alkali-doped polybenzimidazole membrane. *Int J Hydrogen Energy* 2013;38:10602–6.
- [24] Chen R, Zhao TS. Mathematical modeling of a passive-feed DMFC with heat transfer effect. *J Power Sources* 2005;152:122–30.
- [25] Shah AA, Singh R, Ponce de Leon C, Wills RG, Walsh FC. Mathematical modeling of direct borohydride fuel cells. *J Power Sources* 2013;221:157–71.
- [26] Xu C, Zhao TS, Ye Q. Effect of anode backing layer on the cell performance of a direct methanol fuel cell. *Electrochim Acta* 2006;51:5524–31.
- [27] Newman J, Thomas-Alyea KE. *Electrochemical systems*. 3rd ed. New York: Wiley; 2004.
- [28] Sousa Jr R, Marques dos Anjos D, Tremiliosi-Filho G, Gonzalez ER, Coutanceau C, Sibert E, et al. Modeling and simulation of the anode in direct ethanol fuel cells. *J Power Sources* 2008;180:283–93.

Nomenclature

- C: Species concentration, mol m⁻³
 D: Diffusivity, m² s⁻¹
 E₀: Theoretical potential/voltage, V
 F: Faraday's constant, A s mol⁻¹
 i: Current density, A m⁻²
 i₀: Exchange current density, A m⁻²
 j: Transfer current density, A m⁻²
 l: Thickness, m
 N: Flux, mol m⁻² s⁻¹
 P: Gas pressure, Pa
 R: Universal gas constant, J mol⁻¹ K⁻¹
 s: Stoichiometric coefficient
 T: Operating temperature, K
 x: Coordinate
 z: Valence of ion

Greek

- α: Transfer coefficient
 ε: Porosity
 γ: Reaction order
 η: Overpotential, V
 σ: Conductivity, Ω⁻¹ m⁻¹

Superscripts

- ACL: Anode catalyst layer
 CCL: Cathode catalyst layer
 eff: Effective
 EtOH: Ethanol

inlet: Inlet
O₂: Oxygen
OH⁻: Hydroxyl ion
ref: Reference

Subscripts

O: Standard
a: Anode

c: Cathode
CH₃COO⁻: Acetate
EtOH: Ethanol
i: Species
M: Membrane
Na⁺: Sodium ion
O₂: Oxygen
OH⁻: Hydroxyl ion